THE JOURNAL OF BIOLOGICAL CHEMISTRY
Vol. 275, No. 38, Issue of September 22, pp. 29458–29465, 2000

Printed in U.S.A.

High and Low Affinity Heparin-binding Sites in the G Domain of the Mouse Laminin α4 Chain*

Received for publication, April 12, 2000, and in revised form, June 26, 2000
Published, JBC Papers in Press, July 11, 2000, DOI 10.1074/jbc.M003103200

Hirotake Yamaguchi‡§, Hironobu Yamashita‡§, Hitoshi Mori‡, Ikuko Okazaki¶, Motoyoshi Nomizu¶, Konrad Beck‖, and Yasuo Kitagawa‡ ‡‡**

From the ‡Graduate Course for Regulation of Biological Signals, Graduate School of Bioagricultural Sciences and ‖Bioscience Center, Nagoya University, Nagoya 464-8601, Japan and the ¶Graduate School of Environmental Earth Science, Hokkaido University, Sapporo 060-0810, Japan

G domains of the mouse laminin α1 and α4 chains consisting of its five subdomains LG1–LG5 were overexpressed in Chinese hamster ovary cells and purified by heparin chromatography. α1LG1–LG5 and α4LG1–LG5 eluted at NaCl concentrations of 0.30 and 0.47 M, respectively. In solid phase binding assays with immobilized heparin, half-maximal concentrations of 14 (α1LG1–LG5) and 1.4 nM (α4LG1–LG5) were observed. *N*-Glycan cleavage of α4LG1–LG5 did not affect affinity to heparin. The affinity of α4LG1–LG5 was significantly reduced upon denaturation with 8 M urea but could be recovered by removing urea. Chymotrypsin digestion of α4LG1–LG5 yielded high and low heparin affinity fragments containing either the α4LG4–LG5 or α4LG2–LG3 modules, respectively. Trypsin digestion of heparin-bound α4LG1–LG5 yielded a high affinity fragment of about 190 residues corresponding to the α4LG4 module indicating that the high affinity binding site is contained within α4LG4. Competition for heparin binding of synthetic peptides covering the α4LG4 region with complete α4LG1–LG5 suggests that the sequence AHGRL1521 is crucial for high affinity binding. Introduction of mutation of H1518A or R1520A in glutathione *S*-transferase fusion protein of the α4LG4 module produced in *Escherichia coli* markedly reduced heparin binding activity of the wild type. When compared with the known structure of α2LG5, this sequence corresponds to the turn connecting strands E and F of the 14-stranded β-sheet sandwich, which is opposite to the proposed binding sites for calcium ion, α-dystroglycan, and heparan sulfate.

Basement membranes are sheet-like extracellular matrices underlying epithelial and endothelial cells, surrounding muscle cells, adipocytes, and peripheral nerve axons, and acting as supportive architecture for the cells to proliferate, differentiate, and migrate. These matrices contain one or more members of the laminin family as a major component. The laminins consist of heterotrimeric (αβγ) glycoproteins, and five α, three β, and three γ subchains have been recognized to combine into more than 11 heterotrimeric molecules identified so far (1–7). The best characterized laminin-1 (α1β1γ1) is a cross-shaped molecule in which all three chains contribute to the α-helical coiled-coil to form the long arm of the cross, whereas the short arms are composed of one chain each (8). Since the N-terminal short arm region is truncated in α3 (splice variant of α3A), α4, β3, and γ2, we can define three groups of laminins; the cross-shaped laminins containing a complete complement of domains (laminins-1, -2, -3, -4, -10, and -11), the rod-shaped laminins lacking domains in all three short arms (laminin-5), and the Y-shaped laminins lacking an α chain short arm but remaining full-sized β and γ chains (laminins-6, -7, -8, and -9). Laminin-1, -2, and -4 form polymers by reversible self-assembly of monomers at short arms in a calcium ion- and temperature-dependent manner with a critical concentration of assembly of 70–140 nM (9–11). This polymerization of the cross-shaped laminins has a central role in forming the meshwork architecture of basement membranes. Since all three short arms are required for self-assembly (11), the laminins lacking either of three short arms cannot contribute to the architecture.

Compared with β and γ chains, all α chains are unique in that their C termini contain a tandem of five laminin G-like (LG)[1] modules, which form a large globular structure at the C-terminal end of laminins and contains binding sites for heparin (12) and α-dystroglycan (13, 14). Taking advantage of recombinant G domain overexpressed in cultured cell lines, their functional regions have been characterized for α1, α2, and α5 (15–21). Recent crystallography of the mouse α2LG5 revealed a 14-stranded β-sheet sandwich structure, in which a calcium ion-binding site is mapped at one edge of the sandwich surrounded by the residues implicated in heparin and α-dystroglycan binding (22). Crystal structure of the α2LG4–LG5 pair showed that they are arranged in a V-shaped fashion related by a 110° rotation to locate two calcium ion-binding sites 65 Å apart at the tips of the domains opposite the polypeptide termini where they have contacting interface (23).

Laminin α4 lacks the N-terminal short arm and shows an expression pattern distinct from that of the full size α chains. It is expressed in the cell of mesenchymal origin such as endothelial cells (24–27) and mouse 3T3-L1 adipocytes (28, 29). Studies on developing mice showed α4 mRNA to be detectable at embryonic day 7 and peaked at day 15 (30). In adult tissues,

* This work was supported by Grant-in-Aids 09460046 and 11460154 for Scientific Research from the Ministry of Education, Science, Culture and Sports of Japan (to Y. K.). The costs of publication of this article were defrayed in part by the payment of page charges. This article must therefore be hereby marked "*advertisement*" in accordance with 18 U.S.C. Section 1734 solely to indicate this fact.

§ These authors contributed equally to the results of this work.

** Visiting research professor supported by the Ministry of Education, Science, Culture and Sports of Japan.

‡‡ To whom correspondence should be addressed: Graduate School of Bioagricultural Sciences, Nagoya University, Furo-cho, Chikusa-ku, Nagoya-shi 464–8601, Japan. Tel./Fax: 81-52-789-5227; E-mail: i45073a@nucc.cc.nagoya-u.ac.jp.

[1] The abbreviations used are: LG, laminin G-like domain; CHO, Chinese hamster ovary; kb, kilobase(s); nt, nucleotide(s); BSA, bovine serum albumin; DHFR, dihydrofolate reductase; *dhfr*, DHFR gene; GST, glutathione *S*-transferase; PBS, phosphate-buffered saline; PNGase F, peptide-N^4-(acetyl-β-glucosaminyl)-asparagine amidase; RT-PCR, reverse transcription-polymerase chain reaction; Tricine, *N*-[2-hydroxy-1,1-bis(hydroxymethyl)ethyl]glycine.

the expression was localized mainly in mesenchymal cells of lung, cardiac, and skeletal muscle fibers, and immunohistology detected laminin α4 antigen in capillary basement membranes as well as perineurium (30).

Since truncation of N-terminal short arm and characteristic expression patterns suggest distinct activity of the α4 G domain from those of α1 and α2, we have overexpressed mouse α4LG1–LG5 in *dhfr*-deficient CHO cells and compared its heparin binding activity with that of α1LG1–LG5 overexpressed in parallel. We report here that α4LG1–LG5 has stronger affinity to heparin than α1LG1–LG5. While the region spanning α4 LG2–LG3 had affinity comparable to α1LGs, α4LG4 was found to be responsible for the strong binging to heparin.

MATERIALS AND METHODS

Plasmid Construction—Plasmids for the expression of recombinant mouse laminin α1LG1–LG5 and α4LG1–LG5 (Fig. 1) were constructed based on the pEF series of plasmids (31, 32) which have laminin chain cDNA sequences inserted between the signal sequence of erythropoietin receptor for the delivery of the products to the secretory pathway and a c-Myc sequence for epitope tagging. For pEFα4Gmyc, mouse laminin α4cDNA clones isolated from a mouse heart cDNA library constructed in λZAPII (Stratagene) were used. These included pA4-3 (covering the 1.4-kb fragment between nt 4261 and poly(A) tail; nucleotide numbers according Ref. 33), pA4-8 (1.4 kb, nt 3658–5021), pA4–14 (1.9 kb, nt 2714–4611), and pA4–15 (2.5 kb, nt 840–3315). The 0.7-kb *Eco*RI-*Xba*I fragment of pA4-8 and the 1.4-kb *Sac*I-*Eco*RI fragment of pA4-14 were connected at the *Eco*RI end and subcloned in *Sac*I and *Xba*I sites of pBluescript SK$^+$ to generate pBSA4Sac/Xba. A cDNA fragment corresponding to nt 4954–5445 was prepared by PCR using pA4-3 as template and a reverse primer tagged with an extra 5′ *Eco*RV sequence. The resulting fragment was digested with *Xba*I and *Eco*RV, and subcloned into *Xba*I and *Eco*RV sites of pBSA4Sac/Xba to yield pBSA4Sac/*Eco*RV. A cDNA fragment nt 2497–2758t was prepared by PCR using pA4–15 as template and a forward primer tagged with an extra 5′ *Sma*I sequence. The resulting fragment was connected to the *Sac*I-*Eco*RV fragment in pBSA4Sac-*Eco*RV after digestion with *Sma*I and *Sac*I and inserted to *Sma*I and *Eco*RV sites of the pEFΔβ1S to generate pEFα4Gmyc. The sequence was confirmed to code for the mouse α4LG1–LG5 sequence from Gly^{833} to Ala^{1815} followed by a Myc-tag sequence. For construction of pEFα1Gmyc, a cDNA fragment coding for the mouse laminin α1 sequence (34) from Ile^{2100} to Pro^{3060} was prepared by RT-PCR using total RNA extracted from mouse embryonal carcinoma F9 cells and forward and reverse primers tagged with extra 5′ *Bam*HI and *Eco*RV sequences, respectively. The laminin β1 fragment in pEFEΔβ1S was replaced by this fragment at *Bam*HI and *Eco*RV sites to generate pEFα1Gmyc.

α4LG4 module was expressed also in *Escherichia coli* as a GST fusion protein. For this, a cDNA fragment corresponding to nt 4357–4908 was prepared by PCR of pEFα4myc using a forward primer tagged with an extra 5′ *Bam*HI sequence and a reverse primer tagged with an extra 5′ *Eco*RI sequence. The amplified fragment was digested with *Bam*HI and *Eco*RI and inserted into corresponding sites of pGEX-2T (Amersham Pharmacia Biotech). Site-directed mutagenesis was accomplished with Quick Change Site-directed Mutagenesis Kit (Stratagene). For H1518A mutation, paired primers of 5′-CTGTTCTTGGCCGCGGGTCGCTTGGTC-3′ and 5′-GACCAAGCGACCCGCGGCCAAGAACAG-3′ were used. For R1520A mutation, paired primers of 5′-CCTGTTCTTGGCCCATGGTGCGTTGGTCTTTATGTTTAATG-3′ and 5′-CATTAAACATAAAGACCAACGCACCATGGGCCAAGAACAGG-3′ were used.

Cell Culture—*dhfr*-deficient CHO DG44 cells (provided by Dr. Lawrence Chasin, Columbia University, New York) were used for overexpression of mouse α1LG1–LG5 and α4LG1–LG5 domains. Cells were maintained in α-minimal essential medium containing nucleosides and deoxynucleosides, and supplemented with 10% fetal calf serum and antibiotics. Once the stable transfectants were established, α-minimal essential medium without nucleosides and deoxynucleosides was used. To check for *N*-glycosylation of G domains, cells were allowed to attach to culture dishes, washed with Dulbecco's modified PBS, and fed with fresh medium containing 10 μg/ml tunicamycin. After 12 h, cell lysates and conditioned media were analyzed by immunoblot using antiserum against c-Myc (Santa Cruz Biotechnology, sc-789).

DNA Transfection and Selection for Stable Transfectants—Cells were transfected with the plasmids together with pGEMSVdhfr encoding a DHFR minigene (provided by Dr. Hiroshi Teraoka, Shionogi Research Laboratory, Osaka, Japan) by calcium-phosphate precipitation. Selection for stable transfectants and subsequent amplification of the introduced cDNA were carried out as described (35). Expression levels of recombinant G domains were monitored by dot immunoassay of conditioned media with antiserum against c-Myc.

Purification of α1 and α4 G Domains—Conditioned medium (about 500 ml each) of α1LG1–LG5 or α4LG1–LG5 expressing cells was harvested and centrifuged at 1000 × *g* for 10 min to remove cell debris. The supernatant was adjusted to 0.5 mM *N*-ethylmaleimide, and applied to a 5-ml heparin affinity column (HiTrap, Amersham Pharmacia Biotech; 3 ml/min) equilibrated in 10 mM Tris-Cl (pH 7.4), 150 mM NaCl, 2 mM EDTA, 0.5 mM *N*-ethylmaleimide (buffer A). For efficient binding, the flow-through was recycled about 5 times. Elution was carried out on a FPLC system (Amersham Pharmacia Biotech). The column was washed with 30 ml of buffer A, eluted at 0.5 ml/min with a 150-ml linear gradient of 150 to 600 mM NaCl in buffer A, and 2.5-ml fractions were collected. Protein concentration in the fractions was determined with the BCA assay (Pierce) with BSA as standard. Purity and amount of recombinant protein was monitored by SDS-gel electrophoresis in 8% acrylamide gels under reducing conditions (20-μl aliquots). Pure fractions were combined, concentrated up to 0.4 mg/ml, and desalted using Centriprep-30 concentrators (Amicon). 500 ml of medium yielded about 3 mg of purified α1LG1–LG5 or α4LG1–LG5.

Urea De- and Renaturation of α4LG1–LG5 Bound to Heparin—Three 1-ml HiTrap heparin columns A, B, and C were equilibrated with 10 mM Tris-Cl (pH 7.4), 2 mM EDTA (buffer B) and loaded with 0.3 mg each of purified α4LG1–LG5. After washing with 3 ml of buffer B, column A was further washed with 3 ml of buffer B while the others were washed with 3 ml of buffer B containing 8 M urea. Columns A and C were then washed with 3 ml of buffer B while column B was washed with 3 ml of buffer B containing 8 M urea. Elution was performed on a FPLC system (0.1 ml/min) with a 30-ml linear gradient from 0 to 800 mM NaCl in buffer B for columns A and C, and in 8 M urea containing buffer B for column B. Proteins of 1-ml fractions were precipitated by 10% (w/v) trichloroacetic acid, pellets were washed with acetone, and dissolved in SDS sample buffer.

Proteolytic Fragmentation of α4LG1–LG5—Purified α4LG1–LG5 (1.2 mg) was digested at 37 °C with 1-chloro-3-tosylamido-7-amino-2-heptanone-treated α-chymotrypsin (Sigma C-3142) or L-1-tosylamido-2-phenylethyl chloromethyl ketone-treated trypsin (Sigma T-8642) at a 1:50 enzyme/substrate ratio for 2 h. Digestion was stopped by addition of phenylmethylsulfonyl fluoride to a final concentration of 1 mM. The digest was applied to a 1-ml Hi-trap heparin column. The column was washed with 6 ml of buffer A, bound protein was eluted on a FPLC system with a 30-ml linear gradient from 150 to 700 mM NaCl in buffer A, and 1-ml fractions were collected. For SDS-gel electrophoresis, fractions were precipitated with trichloroacetic acid as described above.

Alternatively, digestion with trypsin was carried out after binding to a heparin column. Purified α4LG1–LG5 (0.4 mg) was bound to a 1-ml heparin column, and 15 μg of trypsin dissolved in 1 ml of 50 mM Tris-Cl (pH 7.4), 100 mM NaCl, 2 mM $CaCl_2$ was applied to the column. The column was incubated for 2 h at 37 °C and connected to a FPLC system. After washing with 6 ml of buffer A, the column was eluted (0.1 ml/min) with a 25-ml linear gradient from 150 to 600 mM NaCl in buffer A, and 1-ml fractions were collected. For Tricine-gel electrophoresis, fractions were precipitated with trichloroacetic acid as described.

Microsequencing of Proteolytic Fragments—After electrophoresis, separated peptides were transferred onto polyvinylidene difluoride membranes and stained with Coomassie Brilliant Blue G-250. Corresponding parts of the membrane were cut out, and the peptides were sequenced from the N terminus (36).

Digestion with PNGase F—*N*-Glycans of α4LG1–LG5 were cleaved with PNGase F (BioLabs) according to the manufacturer's instructions. 15 μl of enzyme solution and 30 μl of × 10 G7 buffer (500 mM sodium phosphate buffer, pH 7.5) were added to purified protein (75 μg in 250 μl) and incubated at 37 °C overnight. As a control, 15 μl of water instead of the enzyme solution was used on a separate sample. After appropriate dilution, the digest was directly used for immunoblot and heparin binding analysis.

α1LG1–LG5 and α4LG1–LG5 Binding to Solid-phase Heparin—Solid-phase assays were carried out as described with slight modification (37). Multiwell plates (96 wells; Nunc) were incubated with 10 μg/ml heparin-BSA (Sigma) in 15 mM Na_2CO_3, 35 mM $NaHCO_3$ (pH 9.2), and 3 mM NaN_3 as the first ligand for 18 h at 4 °C. Wells were then blocked with 1% (w/v) BSA in 50 mM Tris-Cl (pH 7.4), 150 mM NaCl, 5 mM $CaCl_2$ (blocking buffer) at room temperature for 2 h. After washing five times with 0.04% Tween 20 in PBS (10 mM Na_2HPO_4, 2 mM K_2HPO_4, 140 mM NaCl, and 3 mM KCl; washing buffer), wells were incubated with α1LG1–LG5 or α4LG1–LG5 serially diluted with blocking buffer as the

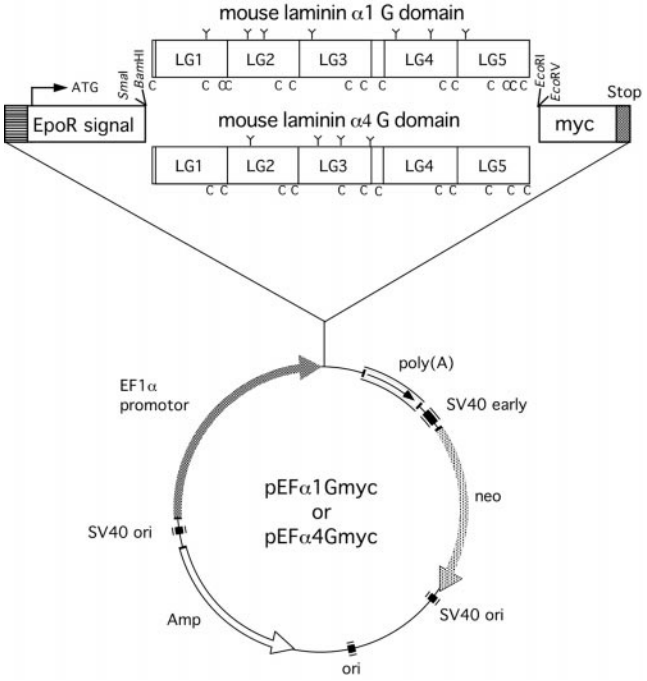

FIG. 1. **Plasmids encoding *α*1LG1–LG5 or *α*4LG1–LG5 sequences.** Map of pEFα1Gmyc and pEFα4Gmyc and the strategy of plasmid construction are summarized. Expression was under the control of the elongation factor 1α (EF1α) promoter. The cDNA sequence encoding mouse α1LG1–LG5 or α4LG1–LG5 was inserted between cDNA sequences of the erythropoietin receptor (EpoR) signal sequence for the delivery of products to the secretory pathway and c-*myc* for epitope tagging. The modular structure of the G domains is schematically shown with *Y*-shaped symbols and letters *C* indicating the approximate positions of *N*-glycosylation sites and cysteine residues, respectively.

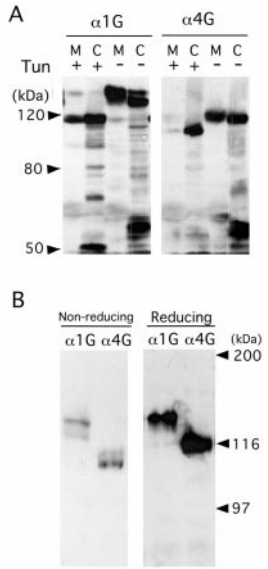

FIG. 2. ***N*-Glycosylation and intrachain disulfide bonding of *α*1LG1–LG5 and *α*4LG1–LG5.** *A,* cells overexpressing α1LG1–LG5 (α1G) or α4LG1–LG5 (α4G) were allowed to attach to culture dishes, washed with Dulbecco's modified PBS and fed with fresh media with (+) or without (−) 10 mg/ml tunicamycin. After 12 h, cell lysates (*C*) and conditioned medium (*M*) were separated by SDS electrophoresis in 12% acrylamide gels under reducing conditions and immunoblotted with antiserum against c-Myc. *B,* conditioned medium was separated by SDS electrophoresis in 12% acrylamide gels under non-reducing and reducing conditions and immunoblotted with antiserum against c-Myc. Positions of size markers are indicated by *arrowheads*.

second ligand. After incubation for 2 h at 4 °C, wells were washed five times with washing buffer, and the bound G domain was incubated with antiserum against α1LG1–LG5, α4LG1–LG5, or c-Myc with dilutions of 1:1000, 1:1000, or 1:400, respectively. After washing five times with washing buffer, bound antibodies were detected with horseradish peroxidase-conjugated goat anti-rabbit IgG (Amersham Pharmacia Biotech) followed by addition of 0.4 mg/ml *o*-phenylenediamine dihydrochloride (Sigma) dissolved in 50 mM phosphate citrate buffer and 0.01% H_2O_2. The reaction was stopped with 3 M HCl. Color yields were determined at 492 nm in a Microplate Reader (Bio-Rad, Model 3550-UV).

Competition Assay of Synthetic Peptides with α4LG1–LG5 for Heparin Binding—One-hundred and 16 peptides (A4G1–116) covering α4LG1–LG5 were designed according to the deduced amino acid sequenced in Ref. 33. Twenty-four peptides (A4G74–97) corresponding to α4LG4 module and two control peptides (A4G82S and A4G82T) were synthesized by the 9-fluorenylmethoxycarbonyl (Fmoc) strategy and purified by high performance liquid chromatography as described previously (38). Purity and identity of the peptides were confirmed by an analytical high performance liquid chromatography and an ion spray mass spectrometer, respectively. Either of the synthetic peptides (21 μg), α4LG1–LG5 (3.4 μg) and heparin-Sepharose CL-6B beads (1 mg) were mixed in 70 μl of 10 mM Tris-Cl (pH 7.4), 100 mM NaCl. After incubation for 1 h at 4 °C, the mixture was loaded on an open column. Beads were flashed three times with 100 μl of the same buffer. Bound protein was extracted with SDS sample buffer and analyzed by SDS-gel electrophoresis.

Heparin Binding Assay of the Mutants of α4LG4 Module—GST fusion proteins of α4LG4 module and the mutants were extracted from *E. coli* by sonication in a buffer containing 10 mM Tris-HCl (pH 7.4) and 2 mM EDTA. The extract (5 ml) was applied to a heparin-Sepharose CL-6B column of 0.5 ml equilibrated with the same buffer. For efficient binding, the flow-through fraction was reloaded three times. The column was washed with 5 ml of the buffer and eluted with 5 ml each of the buffer containing 100, 200, 400, 500, 600, and 1000 mM NaCl. 10 μl of the fractions was analyzed by immunoblot.

Gel Electrophoresis and Immunoblot Analysis—SDS-gel electrophoresis was performed using 8 or 12% acrylamide gels as described (39). Gels were stained with Coomassie Brilliant Blue R-250. Samples were dissolved in SDS sample buffer with or without 2% (v/v) 2-mercaptoethanol. Tricine-gel electrophoresis was carried out as described (40) followed by staining with Coomassie Brilliant Blue G-250. For immunoblot analysis, proteins were transferred to Hybond ECL nitrocellulose membrane (Amersham Pharmacia Biotech) and the membrane was blocked with 5% (w/v) skim milk in PBS (immunoblot blocking buffer) at room temperature for 2 h. After washing five times with 0.1% Tween 20 in PBS (immunoblot washing buffer), the membrane was incubated at room temperature for 2 h with antiserum against α1LG1–LG5, α4LG5, synthetic peptide having the sequence in α4LG5, c-Myc, or GST diluted in immunoblot blocking buffer 1:1000 or 1:400 as the first antibody. After further washing, the membrane was incubated at room temperature for 1 h with horseradish peroxidase-conjugated donkey anti-rabbit IgG (Amersham Pharmacia Biotech) diluted in immunoblot blocking buffer to 1:1000 as the second antibody. ECL Western blotting detection reagents (Amersham Pharmacia Biotech) were used for developing.

Antisera—Antisera against α4LG1–LG5, α4LG1–LG5, and GST were raised by injecting the purified proteins into rabbits. Antiserum against a synthetic peptide LDESFNIGLKFEI (residues 1652–1665 of mouse α4) was raised as described (29).

RESULTS

Overexpression of Mouse α4LG1–LG5 and α4LG1–LG5—*dhfr*-deficient CHO cells were transfected with plasmids encoding the G domains of mouse laminin α1 (α1LG1–LG5) and α4 (α4LG1–LG5) chains, respectively, together with a *dhfr* minigene (pGEMSVdhfr) (Fig. 1). Cells overexpressing and secreting the G domains into the medium were selected among the clones resistant to increasing concentrations of methotrexate by dot-blot immunoassay using anti-c-Myc antiserum.

To test for *N*-glycosylation of α4LG1–LG5 and α4LG1–LG5 in selected clones, media samples and lysates of cells grown in the presence and absence of tunicamycin were analyzed by SDS-gel electrophoresis followed by immunoblotting with antiserum against c-Myc (Fig. 2*A*). Faster migration of the major band of ~120 kDa in the presence of tunicamycin indicates *N*-glycosylation of both α1LG1–LG5 and α4LG1–LG5. When

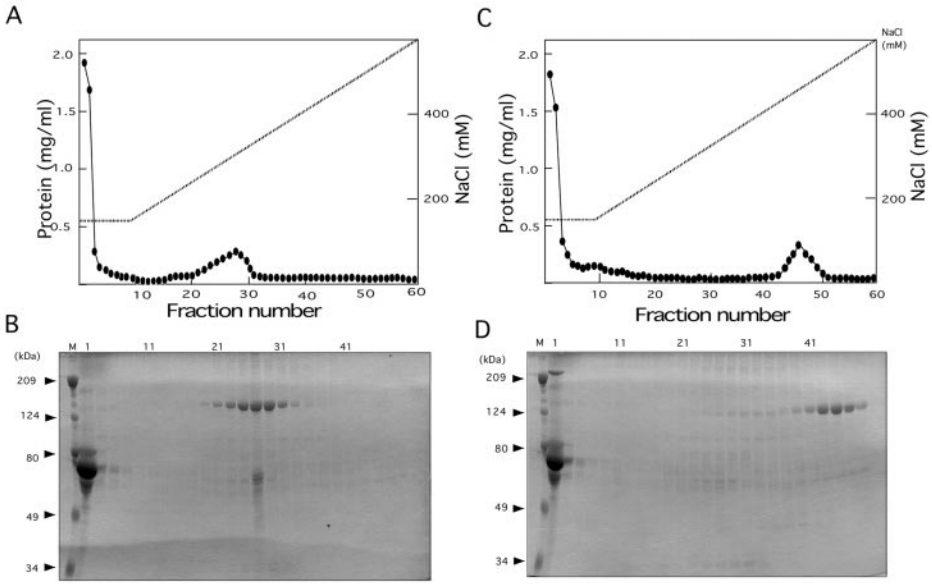

FIG. 3. **Purification of α1LG1–LG5 and α4LG1–LG5 by heparin columns.** Conditioned medium (about 500 ml) of CHO cells expressing α1LG1–LG5 or α4LG1–LG5 was applied to a 5-ml heparin column, the column was washed and eluted with a NaCl gradient (*dashed line* in *A* and *C*). The protein elution profile as determined by the BCA assay (*closed circles*) and SDS gels stained with Coomassie Brilliant Blue of column fractions are shown for α1LG1-LG5 (*A* and *B*) or α4LG1-LG5 (*C* and *D*). Fraction numbers are given at the *top* of the gels. Molecular weight markers (*lane M*) and their size are shown on the *left*.

compared with α4LG1–LG5, the larger migration difference observed for the tunicamycin-treated and untreated α1LG1–LG5 might reflect the different number of potential *N*-glycosylation sites (7 in α1LG1–LG5; 4 in α4LG1–LG5; compare Fig. 1). In contrast to the α1LG1–LG5 expressing cells, tunicamycin treatment of the α4LG1–LG5 expressing cells nearly completely blocked α4LG1–LG5 secretion. Detection of several distinct minor bands migrating faster than the full-length LG1–LG5 modules in the cell lysates suggests intracellular degradation of intermediates. Some degradation was also observed for the secreted proteins. Analysis of conditioned medium by SDS-gel electrophoresis performed under reducing or nonreducing conditions shows an increased mobility of the non-reduced α4LG1–LG5, whereas the migration position of the major part of α1LG1–LG5 remained unaffected (Fig. 2*B*). This suggests a more compact configuration for the oxidized α4LG1–LG5 due to intrachain disulfide bonds, although the upward smear seen in the non-reduced sample could be due to some heterogeneity. The unchanged mobility observed for most of α1LG1–LG5 might indicate incomplete disulfide bond formation; the weak band migrating faster under non-reducing conditions might reflect a minor population with more disulfide bonds.

High Affinity Heparin Binding Activity of α4LG1–LG5—α1LG1–LG5 and α4LG1–LG5 were purified by heparin affinity chromatography. Applying a linear gradient, the α1LG1–LG5 and α4LG1–LG5 eluted at salt concentrations of 300 and 470 mM, respectively, and analysis of column fractions by SDS-gel electrophoresis showed major bands in the migration positions of full-length G domains (Fig. 3). For both proteins, minor bands could bee seen at positions corresponding to about 50–60 kDa which on immunoblots were recognized by α1LG1–LG5- or α4LG1–LG5-specific antisera (not shown). Addition of phenylmethylsulfonyl fluoride to the medium directly after harvesting reduced the amount of these contaminants suggesting that serine protease(s) produced by CHO cells digested the products. The differential heparin affinity of such fragments as especially observed for α4LG1–LG5 suggests that some subdomains contain high and low affinity binding sites.

Binding of G domains to solid-phase heparin confirmed the high affinity of the α4 G domain (Fig. 4). Serially diluted α1LG1–LG5 or α4LG1–LG5 was incubated with heparin bound to the surface of multiwell plates. The concentrations required for half-maximal binding determined with specific antisera

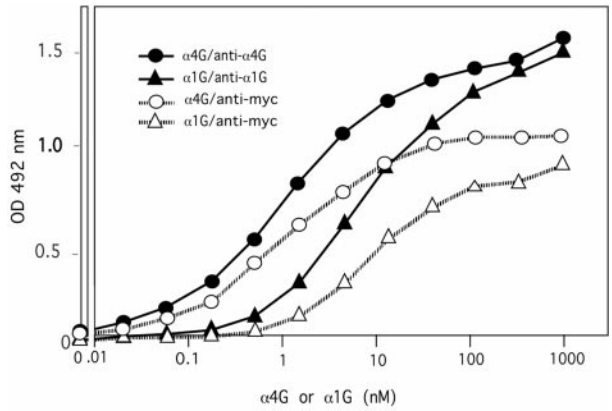

FIG. 4. **Binding of α1 and α4 G domains to solid-phase heparin.** Binding of serially diluted α1LG1–LG5 or α4LG1–LG5 to solid-phase heparin-BSA coated to the surface of multi-well plates was detected by antisera against α1LG1–LG5 (*anti-α1G*), α4LG1–LG5(*anti-α4G*), or Myc tag (*anti-myc*).

were 14 and 1.4 nM for α1LG1–LG5 and α4LG1–LG5, respectively. Antiserum against the c-Myc tag resulted in the same values confirming that the higher affinity of α4LG1–LG5 was not due to different titers of antisera. The half-maximal concentration determined for α1LG1–LG5 is in the same range as previously reported (19). When the same experiments were performed in the presence of 5 mM Ca^{2+}, no measurable changes for heparin affinity were observed for α4LG1–LG5 (data not shown).

Characterization of Heparin Binding Activity of α4LG1–LG5—The results in Fig. 5 show that *N*-glycan in α4LG1–LG5 is not essential for its high affinity binding to heparin. To remove *N*-linked carbohydrates, α4LG1–LG5 was treated with PNGase F. When analyzed by gel electrophoresis, more than 80% of the product migrated in a comparable position as the intracellular precursor produced in the presence of tunicamycin (Fig. 5*A*). Despite the extensive digestion of *N*-glycans, α4LG1–LG5 retained its high affinity to solid-phase heparin indicating that this activity is not mediated by carbohydrates (Fig. 5*B*).

To determine whether the heparin binding activity depends on the native structure of α4LG1–LG5, de- and renaturation experiments with urea were performed. Three heparin columns

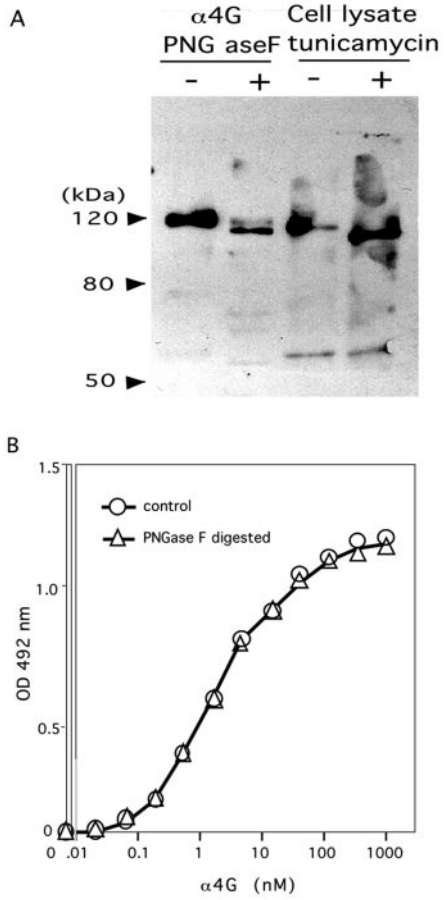

FIG. 5. **Effect of *N*-glycan digestion on heparin binding of α4LG1–LG5.** *A,* α4LG1–LG5 was treated with PNGase F and separated by SDS-gel electrophoresis under reducing condition together with the untreated protein and lysates of cells cultured in the presence or absence of tunicamycin. α4LG1–LG5 was detected by immunoblotting using specific antiserum. *B,* the binding activity of control and PNGase F-treated α4LG1–LG5 to solid-phase heparin was determined as described in the legend to Fig. 4 using antiserum against the Myc tag.

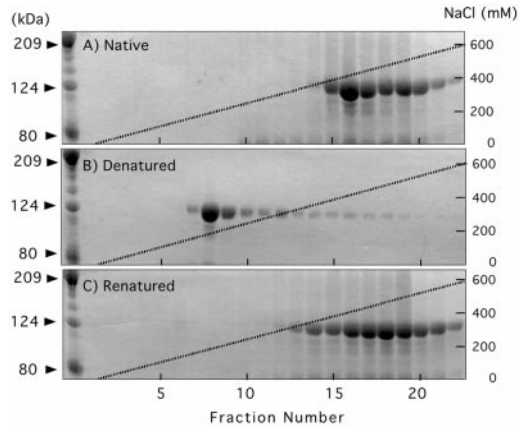

FIG. 6. **Effect of de- and renaturation of α4 G domain on heparin binding activity.** Three heparin columns (*A, B,* and *C*) were loaded with purified α4LG1–LG5. Column A was washed with buffer B whereas columns B and C were washed with buffer B containing 8 M urea. Columns A and C were then washed with 3 ml of buffer B while column B was washed with 3 ml of buffer B containing 8 M urea. Columns were eluted with a 0–800 mM NaCl gradient in buffer B which for column B contained 8 M urea. Gels of fractions from column B show somewhat lower staining intensity which might be due to a lower efficiency of trichloroacetic acid precipitation in the presence of urea.

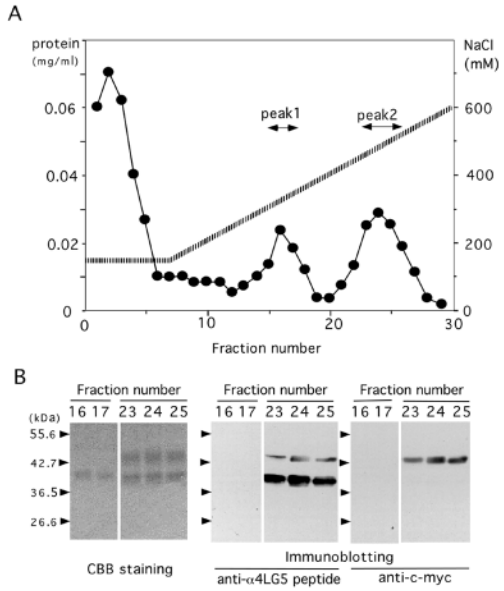

FIG. 7. **High and low affinity heparin binding α4 G chymotryptic fragments.** *A,* α4LG1–LG5 was partially digested with chymotrypsin (enzyme/substrate ratio, 1:50, 37 °C, 2 h) and the digest was applied to a heparin column. Bound protein eluted in two peaks corresponding to an ionic strength of 330 and 480 mM. *Closed circles* and *dotted line* indicate protein and estimated NaCl concentrations, respectively. *B,* peak 1 and peak 2 fractions were analyzed by SDS-gel electrophoresis and stained with Coomassie Brilliant Blue, or were immunoblotted with antiserum against a synthetic peptide of α4LG5 module (anti-α4LG5 peptide) or the c-Myc tag (*anti-c-myc*).

A, B, and C were loaded with equal amounts of protein (Fig. 6). While column A was left under native conditions, columns B and C were washed with 8 M urea. Column C was then washed with a buffer without urea. All three columns were then eluted with a 0 to 800 mM NaCl gradient in the absence (columns A and C) or presence (column B) of 8 M urea. Gel electrophoresis of the column fractions showed that heparin binding activity was reduced to about 180 mM NaCl for column B, but could be nearly completely recovered by the renaturation step used on column C. Although denaturation of α4LG1–LG5 substantially lowers the affinity, it is important to note that the denatured α4LG1–LG5 showed the affinity to heparin.

High and Low Affinity Heparin Binding Subdomains in the α4 G Domain—Endogenous protease(s) of CHO cells appeared to partially degrade α4LG1–LG5 resulting in fragments with different affinity for heparin (Fig. 3*D*). Since this suggests multiple binding sites of different affinity, we tried to dissect α4LG1–LG5 by proteolytic digestion. Both chymotrypsin and trypsin applied at enzyme/substrate ratios of 1/50 for 2 h converted most of the intact α4LG1–LG5 into discrete fragments of 35–45 kDa as determined by SDS electrophoresis. At higher enzyme/substrate ratios, additional smaller fragments could be found. After loading chymotrypsin-digested α4LG1–LG5 on a heparin column equilibrated in 150 mM NaCl, most protein appeared in the flow-through (Fig. 7*A*). Elution with a salt gradient removed two major species at ~330 and ~480 mM NaCl, respectively. SDS electrophoresis of peak 1 showed a single band of 41 kDa whereas peak 2 showed two bands of 44 and 39 kDa (left panel in Fig. 7*B*). Sequencing of the 41-kDa band resulted in TQSRAAS corresponding to a start at residue 1037 suggesting that this fragment contains LG2 and LG3 modules (Fig. 9). Sequencing of the 44- and 39-kDa bands gave the identical sequence KFLEQKE corresponding to a start at residue 1437 which is within a hinge region connecting the LG3 and LG4 modules (Fig. 9). Both fragments thus contain the entire LG4 subdomain. Since the 44-kDa fragment was recognized by anti-c-Myc antiserum (*right panel* in Fig. 7*B*), it covers

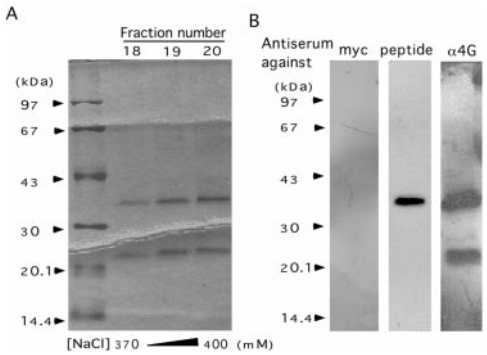

FIG. 8. **High affinity heparin-binding site in α4LG4 module.** *A,* α4LG1–LG5 was bound to a heparin column and digested with trypsin (2 h, 37 °C), eluted with a NaCl gradient from 150 to 600 mM, and 1-ml fractions were collected. Fractions 18–20, corresponding to about 370–400 mM salt, were analyzed by Tricine electrophoresis, and the gel was stained with Coomassie Brilliant Blue. *B,* immunoblots using antiserum against the c-Myc tag (*myc*), the synthetic peptide of α4LG5 (*peptide*) and α4LG1–LG5 (*α4G*) are shown.

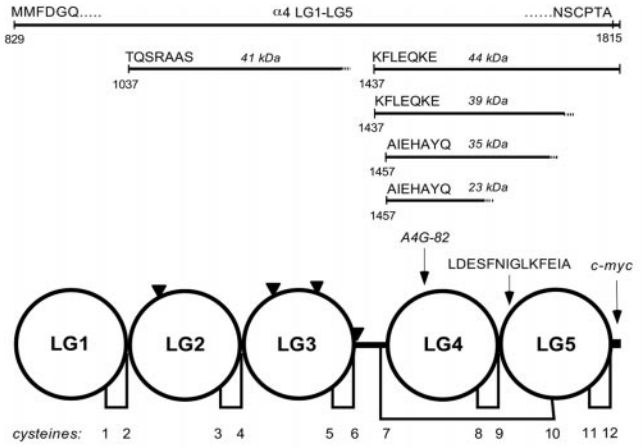

FIG. 9. **Regions of α4LG1–LG5 contained in chymotryptic and tryptic fragments.** The N-terminal sequences and estimated sizes of the chymotryptic and tryptic fragments of are shown aligned to schematic modular structure of α4LG1–LG5 with *triangles* indicating the approximate positions of *N*-glycosylation sites and cysteine residues. The positions of 12 cysteine residues and their estimated disulfide bondings are indicated at the *bottom*.

the sequence down to the C terminus of G domain. The 39-kDa fragment reacted with antiserum against a synthetic peptide LDESFNIGLKFEIA1665 (*middle panel* in Fig. 7*B*) located close to the N terminus of the LG5 module (Fig. 9), but not with anti-Myc (*right panel* in Fig. 7*B*). The size of this fragment suggests that it covers the LG4 module and about 80–90% of the LG5 module (Fig. 9). Despite that the exact cleavage sites were different, parallel analysis of tryptic digests gave quite similar results: two peaks were eluted from the heparin column with one (45 kDa) and two (40 and 35 kDa) bands detected in these peaks. The low and high affinity fragments covered LG2–LG3 and LG4–LG5 modules, respectively (data not shown).

To narrow down the identity of the high affinity binding site, α4LG1–LG5 was bound to heparin beads and extensively digested with trypsin. The heparin bound form was chosen to protect the active configuration. Two fragments of 35 and 23 kDa could be eluted at an ionic strength of about 370–400 mM NaCl (Fig. 8*A*). Both fragments did not react with anti-c-Myc, but they were recognized by anti-α4LG1–LG5 antiserum (Fig. 8*B*). Sequencing of both fragments gave identical N termini of AIEHAYQ corresponding to a start at residue 1457 which is about the begin of LG4 module (Fig. 9). Since the 23-kDa fragment was negative to antiserum against the α4LG5 peptide

A

Peptide	Sequence	Peptide	Sequence
A4G-74	HLFSSPRAIEHA	A4G-85	SQEKYNDGLWHD
A4G-75	IEHAYQYGGTAN	A4G-86	LWHDVIFIREKS
A4G-76	GTANSRQEFEHE	A4G-87	REKSGRLVIDG
A4G-77	FEHEQGDFGEKS	A4G-88	VIDGLRVLEERL
A4G-78	GEKSQFSIRLKT	A4G-89	LEERLPPSGAAW
A4G-79	RLKTRSSHGMIF	A4G-90	GAAWKIKGPIYL
*A4G-80	GMIFYVSDQEEN	A4G-91	GPIYLGGVAPGR
*A4G-81	DQEENDFMTLFL	A4G-92	APGRAVKNVQIT
A4G-82	TLFLAHGRLVFM	*A4G-93	KNVQITSVYSFSG
A4G-82S	GHLLVLMFTARF	*A4G-94	LGNLQLNGASIT
A4G-82T	RHLTLVMFAGLF	*A4G-95	ASITSASQTFSVT
A4G-83	LVFMFNVGHKKL	A4G-96	FEGPMETGTYFS
A4G-84	HKKLKIRSQEKY	*A4G-97	TYFSTEGGYVVL

B

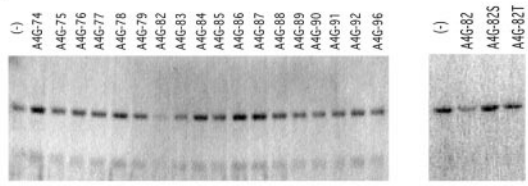

C

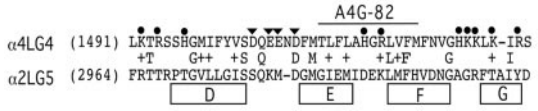

FIG. 10. **Competition of synthetic peptides with α4LG1–LG5 for heparin binding.** *A,* a series of overlapping peptides covering α4LG4 module were synthesized. A4G-82S and -82T contain the same residues as peptide A4G-82 but in scrambled order. The two cysteine residues of the α4LG4 sequence which would be located between A4G-93/94 and A4G-95/96 were omitted. *Asterisks* denote peptides that were insoluble in aqueous solution. *B,* α4LG1–LG5 (~0.4 mM), peptides (~200 mM), and heparin-coated beads were incubated for 1 h at 4 °C, washed, and eluted with SDS sample buffer which was analyzed by gel electrophoresis followed by staining with Coomassie Brilliant Blue. A control sample without peptide is shown in the *left lanes* (−). *C,* the α4LG4 sequence environment of peptide A4G-82 is shown aligned to the mouse α2LG5 module (α2LG5) which high resolution structure has been solved (21). The position of β−strands D to G of α2GL5 is indicated by *boxes*. Basic and acidic residues of α4LG4 are highlighted by *dots* and *triangles*, respectively.

(Fig. 8*B*), it seems to cover the entire LG4 module and perhaps some residues of the LG5 module (Fig. 9). Thus, the 23-kDa fragment was the shortest fragment preserving the high affinity heparin-binding site of α4LG1–LG5. The elution of this fragment from the heparin column at a slightly lower NaCl concentration than that observed for the longer fragments extending more into the LG5 subdomain (Fig. 7) suggests that the sequence within LG5 can support the LG4-binding site.

Competition of Synthetic Peptides within α4LG4 Module for Heparin Binding—To further specify the high affinity heparin-binding site, a series of 24 overlapping 12-mer synthetic peptides were synthesized which cover the sequence region of residues 1450 to 1651 including the entire LG4 module (Fig. 10*A*). Peptides (~200 μM) were added to a mixture of α4LG1–LG5 (~0.4 μM) and heparin-coated beads to find which sequence can compete for the binding of α4LG1–LG5 to heparin. As some peptides (see *asterisks* in Fig. 10*A*) were insoluble in aqueous solvent, they were omitted from the assay. Except for peptide A4G–93, none of them contains any basic residue and thus they are unlikely to cover a heparin-binding site. Only peptide A4G–82 was able to strongly compete for heparin binding with α4LG1–LG5, although A4G-83 showed some weak activity (Fig. 10*B*). This suggests that two basic amino acids (His^{1518} and Arg^{1520}) in the sequence TLFLAHGRLVFM1524 are important for the high affinity binding of the α4 G domain.

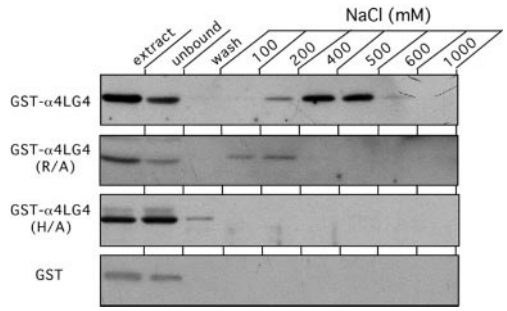

FIG. 11. **Heparin binding activity of GST fusion protein of α4LG4 module having mutation of R1518A or H1520R.** GST fusion protein of α4LG4 (*GST-α4LG4*), its mutant of R1518A (*GST-α4LG4*(*R/A*)), of H1220A (*GST-α4LG4*(*H/A*)) or GST was extracted from *E. coli* of the corresponding clone and loaded to a heparin-Sepharose column. After washing with a buffer containing 10 mM Tris-HCl (pH 7.4) and 2 mM EDTA, the column was eluted stepwise by the same buffer containing the indicated concentration of NaCl. 10 μl of the fractions was separated by SDS electrophoresis using 12% acrylamide gel and the proteins were detected by immunoblot with antiserum against α4LG1–5 or GST.

The inactivity of peptides A4G-82S and -82T consisting of the same amino acids but in a randomly scrambled order indicates the significance of the specific positioning and context of these basic residues. When the peptide concentration was reduced to ~20 μM, the competitive effect of A4G-82 was hardly detectable. This indicates that a more than 50-fold molar excess of peptide was needed to bind to heparin at efficiency comparable to that of α4LG1–LG5.

Heparin Binding Activity of Recombinant α4LG4 Module Having Mutation at His[1518] or Arg[1520]—To confirm the critical role of basic amino acids in peptide A4G-83, we produced a GST fusion protein of α4LG4 module in *E. coli* by constructing a pGEX plasmid harboring cDNA encoding the sequence from Ser[1452] through Pro[1636] with mutation of none, R1518A, or H1520A. pGEX was our choice to extract the product from bacteria by sonication. When the extract from the clone producing wild type α4LG4 fusion protein was applied to a heparin column, one-half of the protein was detected in unbound fraction probably due to overloading, but the least was eluted at NaCl concentration of 400–500 mM (Fig. 11). GST sequence alone showed no affinity to heparin (Fig. 11). This showed that the bacterial system could produce the α4LG4 module with similar configuration as in the CHO system. The affinity was comparable to the 44- and 39-kDa fragments (Fig. 7) but was higher than the 35- and 23-kDa fragment (Fig. 8), suggesting that Arg[1456] may contribute to heparin binding. Mutation of R1518A reduced the affinity and the protein was eluted at NaCl concentrations of 100–200 mM (Fig. 11). Mutation of H1520A showed a more dramatic effect and almost totally ruined the affinity of the α4LG4 module (Fig. 11). We thus found that the sequence of AHGRL1521 was critical for heparin binding.

DISCUSSION

When compared with other laminin G domains so far studied (15–21), α4 G domain shows the highest affinity to heparin. α4LG1–LG5 eluted from a heparin column at a NaCl concentration of 470 mM (Fig. 3*C*) whereas different LG modules of α1 and α2 chains, and the whole α1 G domain were eluted at an ionic strength of 140–360 mM (15, 17, 19). The α1LG1–LG5 prepared by us also eluted at 300 mM NaCl (Fig. 3*A*). In a solid phase binding assay using immobilized heparin, the concentrations of α4LG1–LG5 and α1LG1–LG5 required for half-maximal binding were 1.4 and 14 nM, respectively (Fig. 4). For the α1 G domain, this value is in the same range as reported for various α1 and α2 LG modules (19). The half-maximal concentration of 3 nM reported recently for α5LG4–LG5 (21) was yet higher than we found for α4LG1–LG5. The affinity of α4 G domain is comparable to that found for the high affinity heparin binding type III repeats in fibronectin (41) and for the heparin-binding region present within the triple helical part of the collagen α1(V) chain (42), but lower than the extremely high affinity of lipoprotein lipase (43) and antithrombin III (44). The physiological significance of this high affinity of α4 G domain remains unclear. In laminins containing the full size α chains (α1 and α2), further heparin-binding sites have been mapped to the N-terminal domain (45). As these regions are absent in the truncated α3 (2) and α4 chains (27, 29, 30, 33), an enhanced affinity to heparan sulfate proteoglycans at the C termini might produce a basement membrane architecture different from that suggested for the laminins containing the full-size laminin chains (46).

As shown for α1 G domain (15, 16), trypsin and chymotrypsin digestion of α4LG1–LG5 produced fragments with differential affinity to heparin. Our fragments of low affinity eluting at 330 mM NaCl consisted of LG2–LG3 modules; the high affinity fragments eluting at 480 mM NaCl contained LG4–LG5 modules (Fig. 7). Extensive digestion into the LG4 module slightly reduced its affinity (Fig. 8), but it still retained high affinity comparable to the whole α4LG1–LG5. This indicates that the binding sites are independent and do not cooperate to enhance the affinity to heparin. This is different from the heparin-binding site of antithrombin III, where seven lysine and arginine residues line a 50-Å cannel supported by the whole structure of the molecule (44). In that situation, the key residues can cooperate with each other to produce extremely high affinity requiring 2 M NaCl to be eluted from a heparin column. Digestion of α4LG1–LG5 with PNGase F did not alter the affinity to heparin (Fig. 5*B*). Considering that all putative *N*-glycosylation sites are within LG2–LG3 modules (Fig. 9), however, this does not prove that *N*-glycans are dispensable. Since the affinity of the whole α4LG1–LG5 was determined by the most potential site located within the LG4 module, there remains a possibility that binding of the LG2–LG3 low affinity site to heparin might be affected by the digestion but binding of the whole molecule was supported by the high affinity site within LG4 module.

Treatment of α4LG1–LG5 with 8 M urea reversibly diminished its heparin binding activity (Fig. 6), indicating that binding depends on the local configuration despite the independence of individual binding sites. Since the binding activity could be recovered to the high affinity exerted mainly by LG4 module after withdrawal of urea, the effect of denaturation/renaturation on the binding activity of whole α4LG1–LG5 was expected to reflect the configuration of LG4 module. Notably, weak but distinct affinity to heparin was even retained in the presence of 8 M urea (Fig. 6*B*), suggesting that some affinity is independent of the correct tertiary structure. Based on these observations, we tested the competition of a series of overlapping synthetic peptides covering the entire LG4 sequence for the binding with α4LG1–LG5 to heparin beads. Surprisingly, peptide A4G-82 containing only two basic residues, His[1518] and Arg[1520], specifically competed for binding whereas peptides containing two large basic clusters, namely Lys[1492]-Arg[1494]-His[1497] in A4G-79 and His[1529]-Lys[1530]-Lys[1531]-Lys[1533] in A4G-84, did not show any activity (Fig. 10*B*). Site-directed mutagenesis of the sequence by producing GST fusion proteins of the α4LG4 module in *E. coli* confirmed the critical role of His[1518] and Arg[1520] (Fig. 11). Alignment of α4LG4 sequence with that of the α2LG5 module (Fig. 10*C*) suggests that the peptide A4G-82 sequence relates to the turn between strands E and F

in the recently determined α2LG5 structure (22). Thus, His^{1518} and Arg^{1520} would be extruded at the opposite edge of the 14-stranded β-sheet sandwich structure to where a calcium ion binds. The neighboring basic cluster of His^{1529} to Lys^{1533} represented by peptide A4G-84 would correspond to the turn connecting strands F and G (Fig. 10*C*) close to the calcium ion coordinating center in α2LG5 (20). The α4LG4 module contains a cluster of acidic amino acids Asp^{1506}-Glu^{1508}-Glu^{1509}-Asp^{1511} which matches to the turn between strands D and E (Fig. 10*C*) and would be extruded to the calcium ion binding edge. In our solid-phase binding assay, measurements of the heparin affinity of the α4 G domain showed identical results in the presence and absence of 5 mM Ca^{2+}. The α4LG4 high affinity site for heparin binding is thus opposite to the edge responsible for the interaction with calcium ion, heparin, and α-dystroglycan in α2LG5 (20).

A 500-fold concentration of A4G-82 was needed to observe the competition. This suggested that only a small part of the A4G-82 peptide had the correct configuration of the heparin-binding site. Alternatively, some additional sequence motif adjacent to the E-F turn might be needed for the high affinity heparin binding. The crystal structure of the α2LG5 module predicts that another basic amino acid cluster of Lys^{1492}-Arg^{1494}-His^{1497} at the N terminus of the strand D (Fig. 10*C*) might be adjacent to F-G turn. Although the peptide representing this cluster (A4G-79) alone did not show competitive effect (Fig. 10*B*), we could expect that Lys^{1492}-Arg^{1494}-His^{1497} would cooperate with His^{1518}-Arg^{1520} to organize a high affinity heparin-binding site. Combination of A4G-82 and A4G-79 in the competition assay, however, did not show any synergetic effect on the competition activity of A4G-82 (data not shown).

Crystal structure of the α2LG4 and LG5 module pair showed that the extended N-terminal sequence (the linker sequence between LG3 and LG4 modules) is disulfide bonded to the LG5 module and the paired modules are arranged in a V-shaped fashion related by a 110° rotation to locate two calcium-binding sites 65 Å apart at the tips of the domains opposite the polypeptide termini (23). Because of this extra disulfide bonding, LG5 is likely to be closer in space to the LG1–LG3 portion than LG4. LG4 might be thus extruded from the main body of G domain. Although the edge opposite the calcium ion-binding site comes to the bottom of V-shape arrangement of the modules, the E-F turn is exposed outside of the contacting interface. Thus, the high affinity heparin-binding site suggested in α4LG4 might be located at the tip of entire laminin molecule for facilitated access to other extracellular matrix components. When overlapped on α4G4 sequence, the extra disulfide bonding fond in α2LG4-LG5 pair correspond to a bonding between Cys^{1449} and Cys^{1719} (7th and 10th cysteines in Fig. 9). It is intriguing that the 39-kDa fragment in chymotrypsin disgusts (Fig. 7) contained this putative disulfide bonding whereas the shortest fragments of 35 and 23 kDa in trypsin digests of α4LG1–LG5 bound to heparin (Fig. 8) did not (Fig. 9). Reduced affinity of the latter fragments suggests that the extra disulfide bonding is also important for heparin binding by combining the N-terminal half of LG5 to LG4 module.

REFERENCES

1. Burgeson, R. E., Chiquet, M., Deutzmann, R., Ekblom, P., Engel, J., Kleinman, H., Martin, G. R., Meneguzzi, G., Paulsson, M., Sanes, J., Timpl, R., Tryggvason, K., Yamada, Y., and Yurchenco, P. D. (1994) *Matrix Biol.* **14,** 209–211
2. Ryan, M. C., Tizard, R., VanDevanter, D. R., and Carter, W. G. (1994) *J. Biol. Chem.* **269,** 22779–22787
3. Iivanainen, A., Sainio, K., Sariola, H., and Tryggvason, K. (1995) *FEBS Lett.* **365,** 183–188
4. Miner, J. H., Patton, B. L., Lentz, S. I., Gilbert, D. J., Snider, W. D., Jenkins, N. A., Copeland, N. G., and Sanes, J. R. (1997) *J. Cell Biol.* **137,** 685–701
5. Miner, J. H., Lewis, R. M., and Sanes, J. R. (1995) *J. Biol. Chem.* **270,** 28523–28526
6. Koch, M., Olson, P. F., Albus, A., Jin, W., Hunter, D. D., Brunken, W. J., Burgeson, R. E., and Champliaud, M. F. (1999) *J. Cell Biol.* **145,** 605–618
7. Iivanainen, A., Morita, T., and Tryggvason, K.(1999) *J. Biol. Chem.* **274,** 14107–14111
8. Beck, K., Hunter, I., and Engel, J. (1990) *FASEB J.* **4,** 148–160
9. Yurchenco, P. D., Cheng, Y. S., and Schittny, J. C. (1990) *J. Biol. Chem.* **265,** 3981–3991
10. Yurchenco, P. D., Cheng, Y. S., and Colognato, H. (1992) *J. Cell Biol.* **117,** 1119–1133
11. Cheng, Y. S., Champliaud, M. F., Burgeson, R. E., Marinkovich, M. P., and Yurchenco, P. D. (1997) *J. Biol. Chem.* **272,** 31525–31532
12. Ott, U., Odermatt, E., Engel, J., Furthmayr, H., and Timpl, R. (1982) *Eur. J. Biochem.* **123,** 63–72
13. Ervasti, J. M., and Campbell, K. P. (1993) *J. Cell Biol.* **122,** 809–823
14. Gee, S. H., Blacher, R. W., Douville, P. J., Provost, P. R., Yurchenco, P. D., and Carbonetto, S. (1993) *J. Biol. Chem.* **268,** 14972–14980
15. Yurchenco, P. D., Sung, U., Ward, M. D., Yamada, Y., and O'Rear, J. J. (1993) *J. Biol. Chem.* **268,** 8356–8365
16. Sung, U., O'Rear, J. J., and Yurchenco, P. D. (1997) *Eur. J. Biochem.* **250,** 138–143
17. Sung, U., O'Rear, J. J., and Yurchenco, P. D. (1993) *J. Cell Biol.* **123,** 1255–1268
18. Talts, J. F., Mann, K., Yamada, Y., and Timpl, R. (1998) *FEBS Lett.* **426,** 71–76
19. Talts, J. F., Andac, Z., Göhring, W., Brancaccio, A., and Timpl, R. (1999) *EMBO J.* **18,** 863–870
20. Andac, Z., Sasaki, T., Mann, K., Brancaccio, A., Deutzmann, R., and Timpl, R. (1999) *J. Mol. Biol.* **287,** 253–264
21. Nielsen, P. K., Gho, Y. S., Hoffman, M. P., Watanabe, H., Makino, M., Nomizu, M., and Yamada, Y. (2000) *J. Biol. Chem.* **275,** 14517–14523
22. Hohenester, E., Tisi, D., Talts, J. F., and Timpl, R. (1999) *Mol. Cell* **4,** 783–792
23. Tisi, D., Talts, J. F., Timpl, R., and Hohenester, E. (2000) *EMBO J.* **19,** 1432–1440
24. Tokida, Y., Aratani, Y., Morita, A., and Kitagawa, Y. (1990) *J. Biol. Chem.* **265,** 18123–18129
25. Sorokin, L., Girg, W., Gopfert, T., Hallmann, R., and Deutzmann, R. (1994) *Eur. J. Biochem.* **223,** 603–610
26. Sorokin, L. M., Pausch, F., Frieser, M., Kröger, S., Ohage, E., and Deutzmann, R. (1997) *Dev. Biol.* **189,** 285–300
27. Frieser, M., Nöckel, H., Pausch, F., Röder, C., Hahn, A., Deutzmann, R., and Sorokin, L. M. (1997) *Eur. J. Biochem.* **246,** 727–735
28. Aratani, Y., and Kitagawa, Y. (1988) *J. Biol. Chem.* **263,** 16163–16169
29. Niimi, T., Kumagai, C., Okano, M., and Kitagawa, Y. (1997) *Matrix Biol.* **16,** 223–230
30. Iivanainen, A., Kortesmaa, J., Sahlberg, C., Morita, T., Bergmann, U., Thesleff, I., and Tryggvason, K. (1997) *J. Biol. Chem.* **272,** 27862–27868
31. Niimi, T., and Kitagawa, Y. (1997) *FEBS Lett.* **400,** 71–74
32. Niimi, T., Miki, K., and Kitagawa, Y. (1997) *J. Biochem.* (*Tokyo*) **121,** 854–861
33. Liu, J., and Mayne, R. (1996) *Matrix Biol.* **15,** 433–437
34. Sasaki, M., Kleinman, H. K., Huber, H., Deutzmann, R., and Yamada, Y. (1988) *J. Biol. Chem.* **263,** 16536–16544
35. Kaufman, R. J., Wasley, L. C., Davies, M. V., Wise, R. J., Israel, D. I., and Dorner, A. J. (1989) *Mol. Cell. Biol.* **9,** 1233–1242
36. Matsudaira, P. (1987) *J. Biol. Chem.* **262,** 10035–10038
37. Aumailley, M., Wiedemann, H., Mann, K., and Timpl, R. (1989) *Eur. J. Biochem.* **184,** 241–248
38. Nomizu, M., Kuratomi, Y., Malinda, K. M., Song, S. Y., Miyoshi, K., Otaka, A., Powell, S. K., Hoffman, M. P., Kleinman, H. K., and Yamada, Y. (1998) *J. Biol. Chem.* **273,** 32491–32499
39. Laemmli, U. K. (1970) *Nature* **227,** 680–685
40. Schägger, H., and von Jagow, G. (1987) *Anal. Biochem.* **166,** 368–379
41. Kapila, Y. L., Niu, J., and Johnson, P. W. (1997) *J. Biol. Chem.* **272,** 18932–18938
42. Delacoux, F., Fichard, A., Geourjon, C., Garrone, R., and Ruggiero, F. (1998) *J. Biol. Chem.,* **273,** 15069–15076
43. Hill, J. S., Yang, D., Nikazy, J., Curtiss, L. K., Sparrow, J. T., and Wong, H. (1998) *J. Biol. Chem.* **273,** 30979–30984
44. Ersdal-Badju, E., Lu, A., Zuo, Y., Picard, V., and Bock, S. C. (1997) *J. Biol. Chem.* **272,** 19393–19400
45. Colognato, H., MacCarrick, M., O'Rear, J. J., and Yurchenco, P. D. (1997) *J. Biol. Chem.* **272,** 29330–29336
46. Yurchenco, P. D., and Schittny, J. C. (1990) *FASEB J.* **4,** 1577–1590